Progress In Electromagnetics Research C, Vol. 118, 25–41, 2022

Wide-Band Frequency Tunable Antenna for 4G, 5G/Sub 6 GHz Portable Devices and MIMO Applications

Shivleela Mudda[1, *], Gayathri KM[1], and Mudda Mallikarjun[2]

Abstract—A compact ($25 \times 28 \times 1.57\,\text{mm}^3$) and wide-band multimode frequency tunable antenna with a defected ground structure (FRDGS) for 4G and 5G conformal portable devices and multi-band wireless systems is presented in this article. In a previous study, frequency reconfigurable antenna designs only used the method of adding slots on the patch or ground. In this study, a combination of multiple slots, partial ground, and defective ground structure techniques are utilised to attain the advantages of compactness, wide impedance bandwidth, and steady radiation pattern. Multiple slots on the top layer of the substrate and F-shaped slot etched at the bottom make the proposed antenna. Two PIN diodes are inserted in the F-shaped slot for frequency reconfiguration, allowing the antenna to switch between different resonances. Ansys high frequency structure simulator 15.0v is used to simulate the antenna parameters. This antenna performance is demonstrated using measured and simulated data. The simulated and measured results clearly show that the proposed antenna can switch among six dissimilar resonant frequency bands via various modes of operation across the frequency spectrum from 2.3 to 8.9 GHz. The antenna works in a variety of commercial bands, such as WLAN/Bluetooth (2.4–2.5 GHz), LTE/4G (2.3–2.7 GHz), S-band (2–4 GHz), Radio Navigation (2.7–2.9 GHz), and 5G/sub-6 (3.3–4.9 GHz), according to simulations and experiments. The proposed design features narrowband, wideband, and ultra-wideband properties with a consistent radiation pattern, adequate gain (1.6 to 5.8 dB), and high radiation efficiency (86 to 94%) in a small package. Furthermore, the performance comparison of the proposed antenna with that of the state-of-the-art antennas in terms of compactness, frequency reconfigurability, number of operating bands, and impedance bandwidth demonstrates the novelty of the proposed antenna and its potential application in multiple wireless applications.

1. INTRODUCTION

There has been the advancement of complex applications and standards such as fifth-generation communication (5G), the internet of things (IoT), vehicular communication, and macro data applications [1]. Electronics and wireless communication devices are rapidly evolving to meet the expanding requirements of customers. The fifth-generation (5G) of communication operating in the sub-6 GHz band is aimed at faster and more reliable communication services with enhanced network capacity. The objective of the 5G network is to provide connectivity to every sort of device and any type of application that may benefit from being connected [2]. 5G antennas should be robust and capable of operating over a wide frequency spectrum. It should also be compatible with active long-term evolution (LTE). Compared to the millimeter-wave spectrum, frequencies below 6 GHz make infrastructure construction and future network deployment easy [3, 4]. New Zealand uses 3.4–3.59 GHz as a future band; Australia uses 3.4–3.7 GHz; and the United States has already implemented the 3.5 GHz spectrum as a 5G band [5]. Modern devices can support multiple applications at the same time, such as Wi-Fi, GPS, Bluetooth, and GSM. These applications operate on different frequency

Received 29 November 2021, Accepted 17 January 2022, Scheduled 26 January 2022
* Corresponding author: Shivleela Mudda (rachu1982@gmail.com).
[1] Dayananda Sagar University, Bangalore, India. [2] Sreenidhi Institute of Science and Technology, Hyderabad, India.

bands and necessitate the use of antennas that are designed for each [6]. The problem with a single device serving multiple applications is that the applications require a high data rate or additional bandwidth. The inclusion of separate antennas for various functions makes the device large and bulky. Therefore, a single antenna operating in many modes within the desired band is the prerequisite of current and future generation devices. Multi-band and reconfigurable antennas are the preferable choices for such devices. Multiband antennas radiate frequencies without letting the user pick or hide specific bands. A frequency reconfigurable antenna can operate in a consumer-specified frequency band while avoiding interference with the antenna's other bands. This guarantees the proper utilisation of the frequency spectrum by enabling continual multiple services to end-users [7, 8]. Microstrip antennas play an important role in recent communication systems, specifically in aircraft, missiles, radar, satellites, and telecommunication networks, because of their provocative characteristics and integration simplicity within monolithic microwave integrated circuits (MMIC) [9]. Numerous methods exist to magnify the functionality of traditional microstrip antennas. The most popular one is defected ground structures (DGSs). The benefits of incorporating a DGS are as follows: it reduces the size of the circuit. In comparison to other approaches, it is simple to develop and manufacture. Its analogous circuit is simple to construct. Finally, it improves precision [10].

The most of the reported work on sub-6-GHz antennas is related to reconfigurable antennas, with RF-PIN diode for frequency reconfigurability being extensively studied by researchers to achieve single-band, dual-band, and multiple-band reconfigurable operations. In [11], a small-sized microstrip antenna with a defective ground structure is investigated. To achieve dual-band frequency, an RF-Pin diode is inserted into the defective ground slot. The designed antenna is smaller than a conventional antenna; however, it has a lower resonating frequency ratio. In [12], a frequency tunable antenna for 5G/sub-6 GHz functioning is studied. The design includes two substrates, and reconfigurability is obtained by incorporating four-pin diodes into the DGS. The total dimension of the design is $100 \times 100 \times 5.7\,\text{mm}^3$. This antenna operates over two bands of 2.37–2.67 GHz and 3.39–3.62 GHz. However, because of its three-dimensional structure, it cannot be used in portable devices. Furthermore, it fails to support the whole sub-6 GHz band. In [13], a frequency tunable dual-band antenna for Wi-Fi and WiMAX wearable operations is introduced. The design uses a lumped RLC model element as a switching approach in the radiating element to provide frequency reconfigurability. The proposed antenna reconfigurable frequencies are 2.44 and 3.54 GHz. A wide-band G-structured antenna is examined in [14] to support W-LAN applications. The antenna operates in two modes, with an impedance bandwidth of 22.9 percent at 2.45 GHz and 50.9 percent at 5.60 GHz. In [15], four photodiodes are utilised to obtain a frequency-agile antenna that operates in four modes. The proposed antenna exhibits three narrow bands and one UWB. A frequency reconfigurable antenna is examined in [16], employing MEMS switches, which are widely used in cognitive radio units. The drawback to such a design is that wide use of MEMS causes substantial insertion loss. In [17], a multiband tunable antenna comprising two pin-diodes for advanced portable device applications is designed. It supports eight operating bands over the range of 1.46 to 6.15 GHz. In [18], a multi-band frequency reconfigurable antenna with a defected ground structure (FRDGS) for multi-standard wireless communication systems is discussed. To realise the multi-band frequency of the antenna and improve the antenna design parameters, the ground plane is modified by embedding U-shaped slots with open ends and I-shaped slots with short ends. The presented antenna lacks operational bandwidth, making it unsuitable for modern wireless applications. Papers [19, 20] present a dual-to-tri-band frequency reconfigurable antenna and a dual-band to quad-band frequency reconfigurable antenna, respectively. Although these antenna designs cover a wide frequency range, they are constrained by narrow bandwidth, complex geometrical structures, and a limited number of operational modes. Furthermore, the antenna presented in [19] has the disadvantage of being larger in size. In conclusion, the antennas in [11–20] have complex geometrical structures and narrow operating bandwidths (BW), making them suitable only for narrow-band applications. In certain designs, more than two PIN diodes are used to obtain a greater number of operational bands, which causes an increase in the price, structure complexity, and reflection loss. In a previous study, the frequency reconfigurable antenna design only used the method of adding slots on the patch or ground (DGS). To address the aforementioned shortcomings, in this study, we attempted to combine the addition of slots on the patch with DGS. The objectives of the proposed work can be summarised as follows:

- A challenge for frequency-reconfigurable antennas is achieving miniaturised structures while

maintaining satisfactory radiation performance across the whole operation bandwidth. To solve this issue, the proposed antenna provides notable compactness with added benefits like dual-band and broadband modes with moderate gain, lower return loss, improved efficiency, and consistent radiation operation.

- Planning a reconfigurable antenna with a few switching elements within a small structure remains a problem. As per the authors' knowledge, it uses just two diodes to support the 4G bands, all sub-6 GHz bands, and other UWB bands.

The rest of this paper is structured as follows: The antenna design approach is illustrated in Section 2. Section 3 gives the findings of the software simulation and fabrication comparison as well as a quick comparison with the most recent studies (multiband and reconfigurable antennas) examined in the literature. Section 4 brings the research to a close.

2. THE PROPOSED ANTENNA DESIGN METHODOLOGY

2.1. Design Method

The design of the suggested antenna evolves in stages, as shown in Figures 1(a)–(d). The top view of the proposed antenna is depicted in Figures 1(b)–(c), and the ground view is in Figure 1(d). Initially,

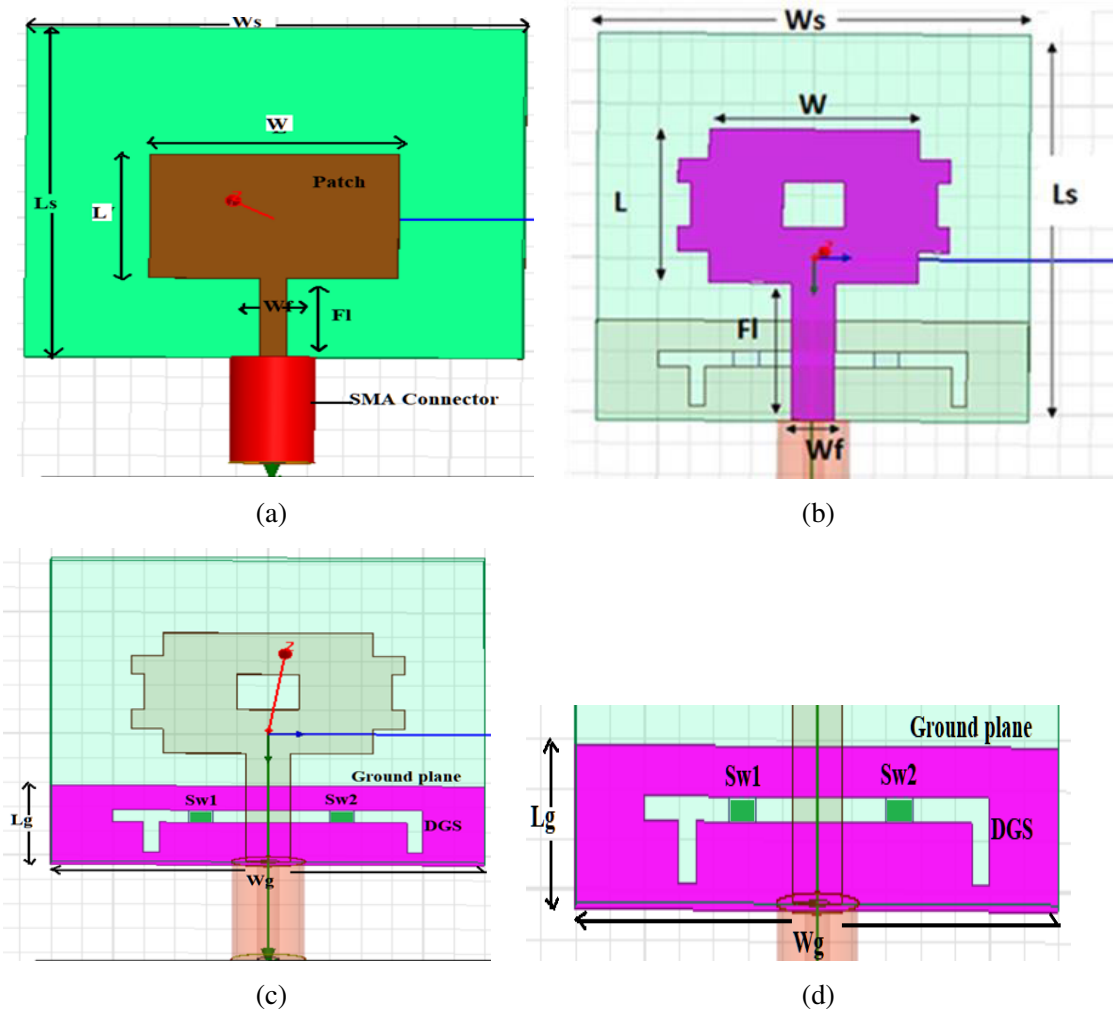

Figure 1. The investigated frequency reconfigurable antenna's geometry. (a) Conventional patch antenna. (b) Front view of the proposed view from the back. (d) Defective ground structure engraved.

the standard microstrip patch antenna is simulated to work at 6.8 GHz, the UWB core frequency. The return loss and VSWR obtained at 6.8 GHz are −11 dB and 1.7, respectively. The antenna of this stage comprises a radiating patch of $9 \times 14\,\text{mm}^2$ and a dielectric substrate of $29 \times 33\,\text{mm}^2$. For normal operation, a microstrip feedline of 50 ohm and an SMA connector linked to the feedline at one end are utilized. The transmission-line model formulae for computing patch, ground, and feed dimensions can be found in [9]. In the second stage, the antenna's computed design values are optimized for compactness. Table 1 shows the optimised dimensions of the patch, substrate height, and ground plane. The compact FRDGS antenna dimension is $25 \times 28 \times 1.57\,\text{mm}^3$ constructed on an FR4 substrate with a dielectric permittivity (ε_r) of 4.2 and a loss tangent of 0.02. Because of its low cost, extensive availability, and strong insulating capacity in both humid and dry situations, FR-4 is preferred.

Table 1. FRDGS antenna's detailed design values.

Variables	Values in mm	Variables	Values in mm
Length of the patch (L)	9.8	Length of feed (F_l)	6
Width of the patch (W)	13.4	Width of feed (W_f)	2.8
Substrate length (L_s)	25	Ground plane slot (L_s)	20
Substrate width (W_s)	28	Ground plane slot ($L_{s1} = L_{s2}$)	1.4
Ground length (L_g)	6.5	Ground plane slot Width	1
Ground width (W_g)	28	Height of substrate	1.57

In the third stage, numerous slots on the patch are engraved to make the antenna multiband. For improved performance, slots are etched at the patch corners and in the maximum current distribution region (see Figure 1(b)). A partial metallic ground plate of $6.5 \times 28\,\text{mm}^2$ dimension is employed to increase bandwidth and to provide an acceptable radiation pattern (refer to Figure 1(c)). In the final stage, a $1 \times 20\,\text{mm}^2$ F-shaped slot is impressed in the partial ground to achieve a defective ground structure. The adoption of DGS improves bandwidth further with dual band characteristics. SMP1320-SC79 PIN diodes are used as switching elements and are placed within the 1 mm slots of the F-shaped DGS to attain frequency reconfiguration (see Figure 1(d)).

2.2. SMP1320-SC79 PIN Diode as an RF Switch

In HFSS, the PIN-diode is modelled as two lumped RLC boundary conditions. After selecting a lumped RLC, the value of resistance (R_S) is selected for the ON state to pose some resistivity, and the value of capacitance (C_T) is declared for the OFF state to pose some capacitance. The analogous circuits for the diode (both ON and OFF states) and the PIN diode model are depicted in Figures 2(a)–(b).

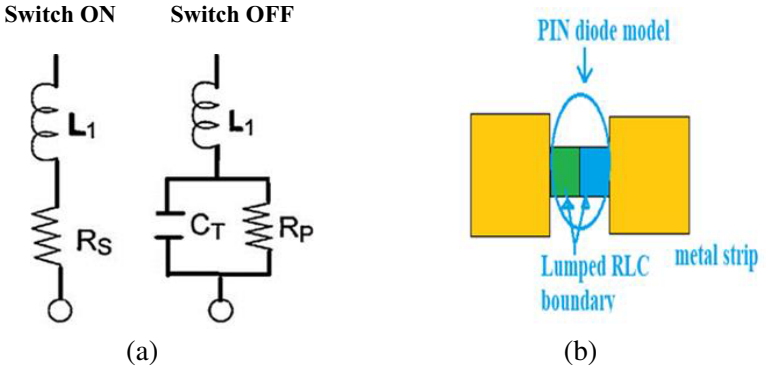

Figure 2. (a) Equivalent circuits for both states of the diode. (b) HFSS simulation model.

The Skyworks Solution, Inc. model SMP-1320-SC79 is the semiconductor switch. The SMP-1320 series features a 0.3 pF capacitance at 5 V and a 0.9-ohm resistance at 10 mA.

2.3. PIN Diode Biasing

The DC biasing circuit and RF antenna circuit must be isolated to some extent. A 100 pF capacitor (package 0603) is used to keep DC from reaching the antenna, and a 33 nH inductor is used to keep RF current from flowing towards the PIN diode (see Figure 3). Table 2 defines the generalised states of the proposed design and the obtained bands.

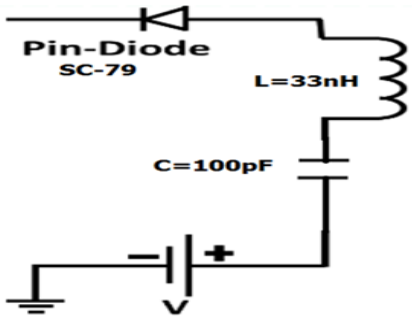

Figure 3. PIN diode biassing circuit.

Table 2. Diode switching configuration details.

Antenna	D1	D2	Frequency Band (GHz)
Mode 1	OFF	OFF	Single Band
Mode 2	ON	OFF	Dual Band
Mode 3	OFF	ON	Dual Band
Mode 4	ON	ON	Wideband

3. SIMULATED AND MEASURED ANTENNA RESULTS

This section deals with the proposed FRDGS antenna performance, in terms of gain, return loss, VSWR, fractional bandwidth, and surface currents. To simulate and analyse the performance of the radiating structure, the High-Frequency Structure Simulator (HFSS) 15.0 version is used.

The Finite Element Method (FEM) is used in HFSS, which makes the design accurate. During simulation, to feed the antenna waveguide port excitation is applied. It is constructed, and a prototype is made to validate the results. The measurements were done with a Keysight Technologies FieldFox Vector Network Analyzer N9926A and an anechoic chamber. Figures 4(a), 4(b), and 4(c) show the measurement setup, and a model of the proposed antenna is built.

3.1. Bandwidth and Return Loss (S-Parameters)

Return loss is measured in decibels (dB), and it must be less than or equal to −10 dB for the antenna to function properly. Figure 5 compares each mode's simulated and measured reflection losses. When switches SW1 and SW2 are turned off in Mode-1, the proposed antenna radiates at 8.05 GHz (single band) with an S_{11} of −11.08 dB and a −10-dB impedance bandwidth of 27.69% (6.9–8.8 GHz). When SW1 is on and SW2 off in Mode-2, the antenna covers dual bands of 2.85 GHz and 7.65 GHz with a return loss of −11.13 dB, −15.60 dB, and −10 dB and bandwidth of 15.38% (2.3–3.3), and 43.03% (6.8–8.8), respectively. In the case of Mode-3, when SW1 is off and SW2 on, the antenna operates at 3 and 7.40 GHz with a return loss of −11.90 dB and −16.54 dB, respectively. In dual bands, the −10 dB

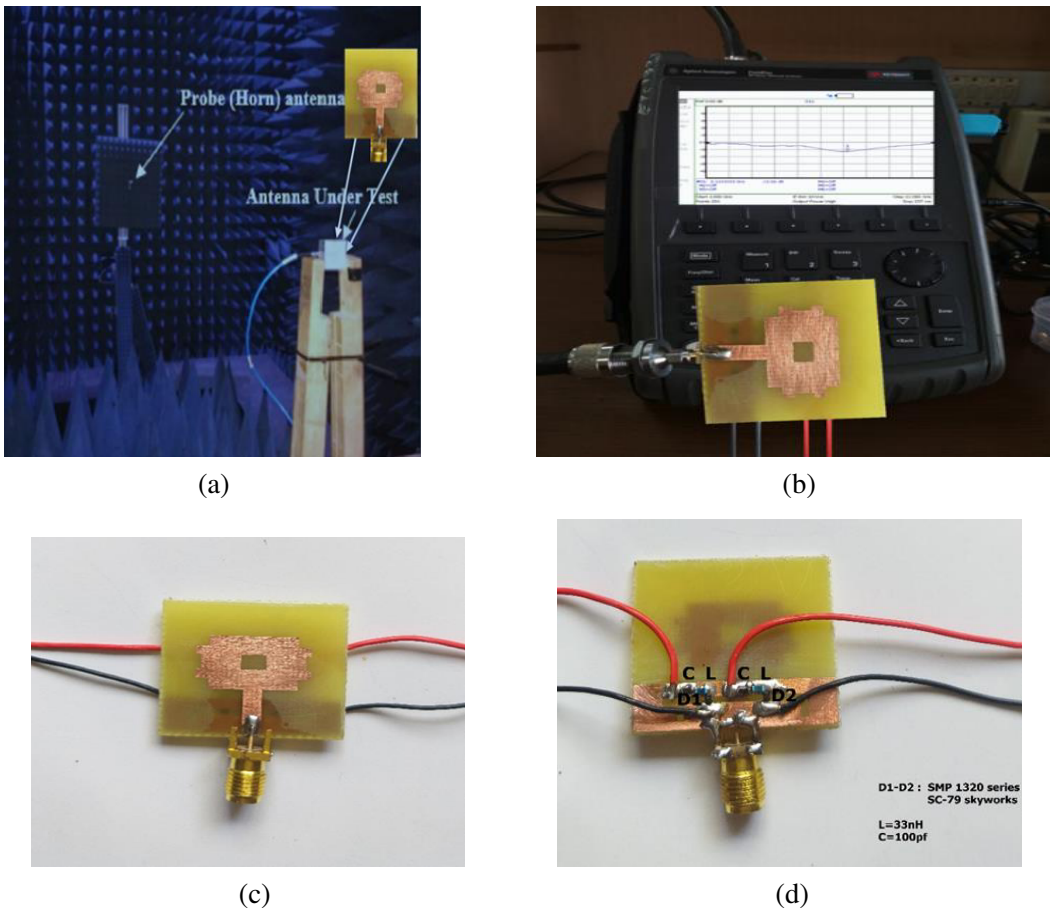

Figure 4. Different views of fabricated antenna: (a) Experimental setup. (b) Measurement setup. (c) Top view. (d) Bottom view with DC-biased lines.

fractional bandwidths are 15.38% (2.4–3.5 GHz) and 43.03% (5.7–8.7 GHz). When both SW1 and SW2 are on, it is tuned to Mode-4 and operates at 5.40 GHz with a return loss of −37.93 dB and a fractional bandwidth of 83.07% (2.4–7.8 GHz). The measured operating frequencies in the four states stated above are 8.10, 2.90/7.70, 3.10/7.50, and 5.45 GHz, with relative bandwidths of 28.69% (6.8–8.9 GHz), 16.76% (2.3–3.3 GHz)/44.30% (6–8.8 GHz), 16.43% (2.3–3.6 GHz)/44.15% (2.4–7.8), and 82.07% (2.4–7.8 GHz). The comparison plots present an acceptable agreement between measured and simulated outcomes.

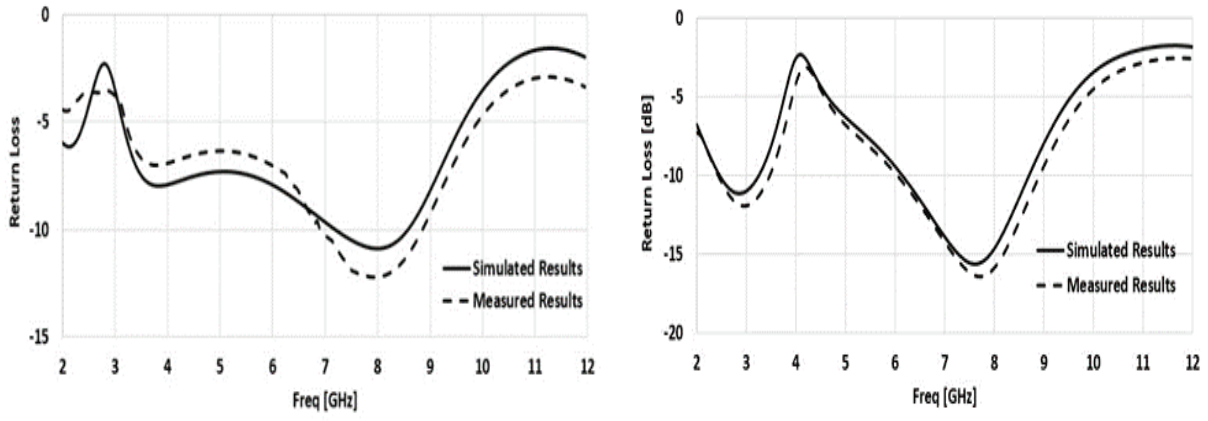

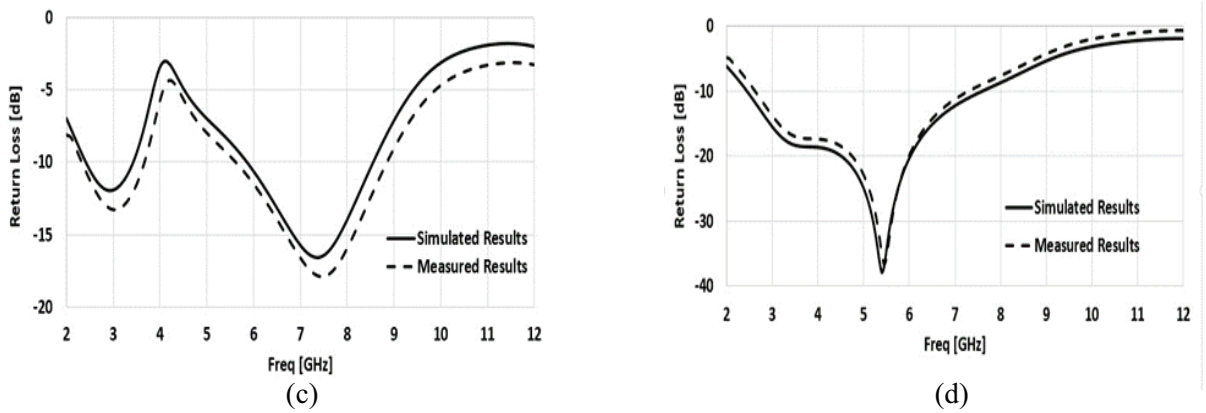

Figure 5. Proposed antenna simulated and measured return loss (S_{11}). (a) Mode 1, (b) Mode 2, (c) Mode 3, (d) Mode 4.

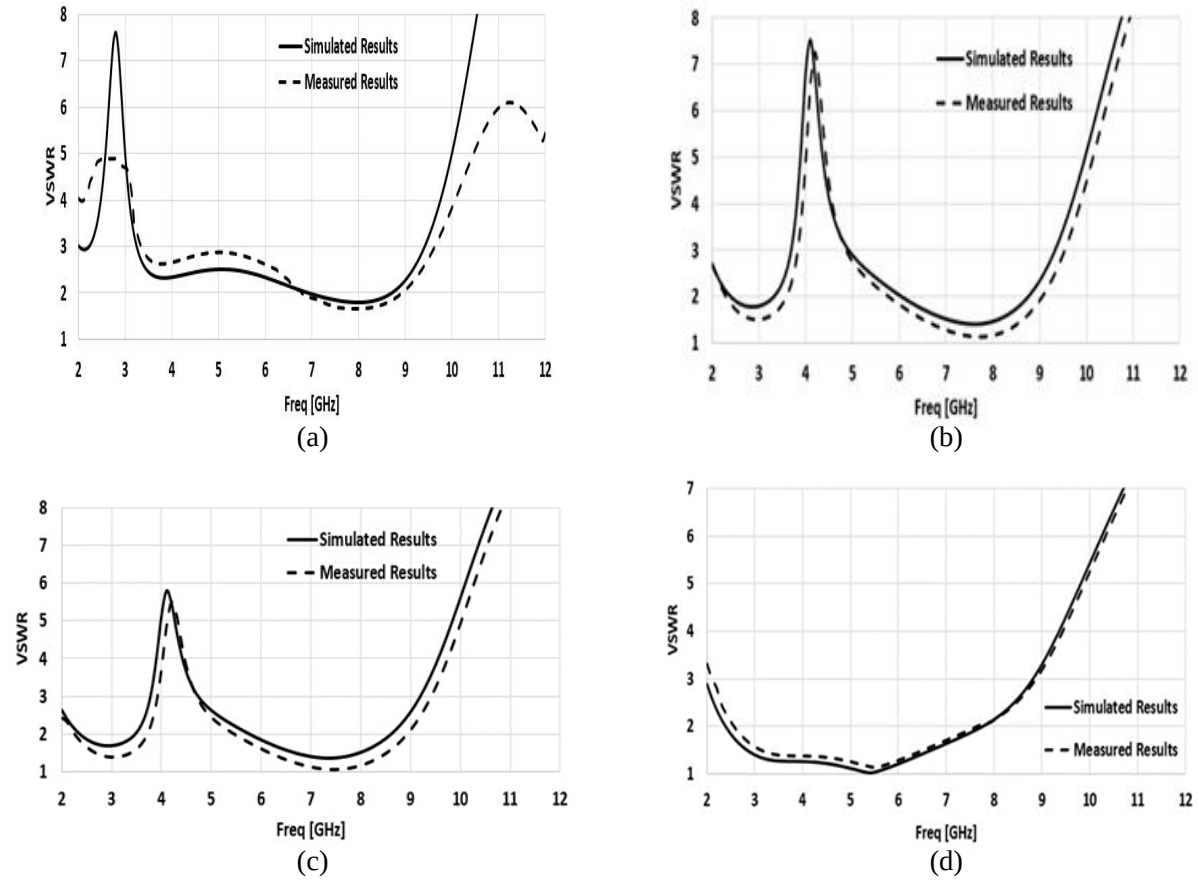

Figure 6. Voltage standing waves ratio of proposed antenna. (a) Mode 1, (b) Mode 2, (c) Mode 3, and (d) Mode 4.

The external biasing circuit and the vector network analyzer cable are to blame for the glitches in the measured result.

Voltage Standing Waves Ratio (VSWR) is another way to express reflection loss. Figure 6 depicts simulated and measured antenna VSWR comparisons. For all resonant bands, the observed VSWR is less than 1.8. It is because of the antenna faultless impedance matching between the source and patch.

The VSWR in mode-4 is nearly equal to 1, making it an ideal candidate for 5G portable devices and sub-6 GHz applications.

3.2. Pattern of Far-Field Radiation

The proposed FRDGS antenna resonates at 8.05 GHz in Mode 1, with a simulated gain of 2.898 dBi and a radiation efficiency of 90.6%. In Mode 2, the antenna radiates at dual bands (2.85 GHz and 7.65 GHz) with peak gains of 1.8 dBi and 2 dBi with radiation efficiencies of 92.6 and 90.2%, respectively. At dual-band frequencies of 3 and 7.45 GHz, the antenna gains and radiation efficiencies are 1.9, 2.4 dBi, and 96.6, 88.7%, respectively. The antenna in Mode 4 resonates at 5.45 GHz with a peak gain of 6.1 dBi and a radiation efficiency of 88.6%. Due to the matched feeding mechanism at the proper position, the suggested antenna has a significant radiation efficiency.

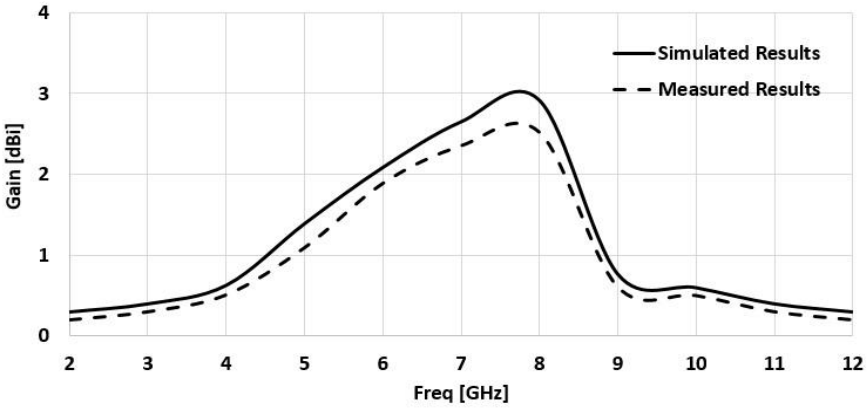

(a)

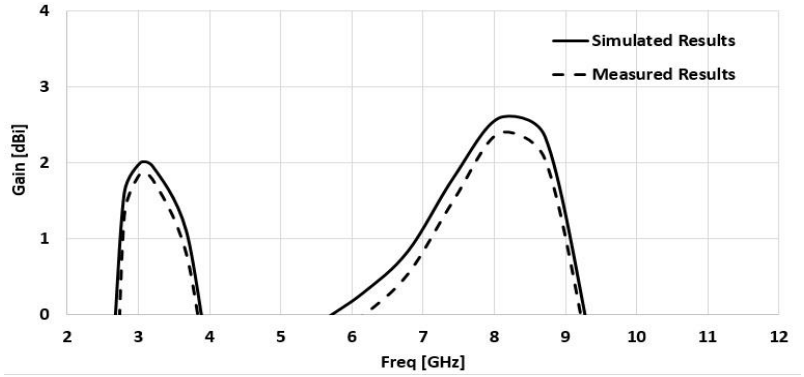

(b)

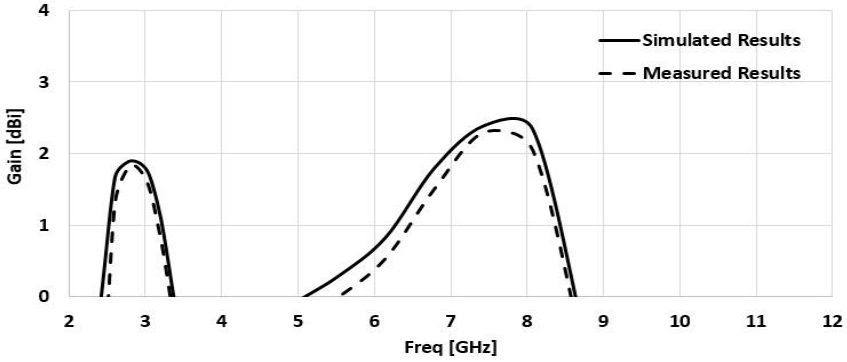

(c)

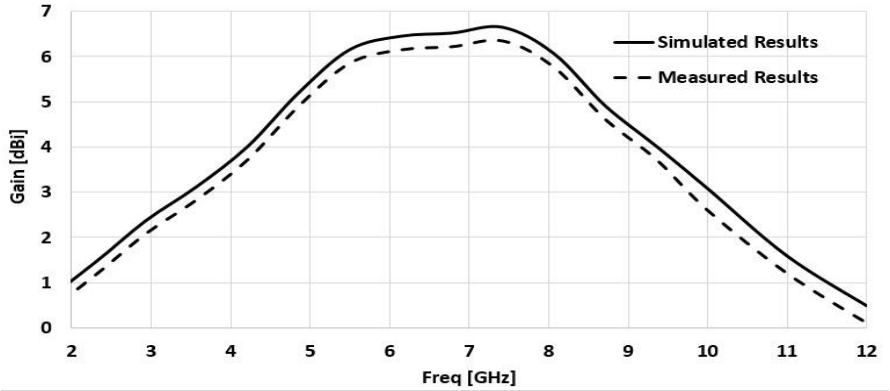

(d)

Figure 7. Proposed antenna simulated and measured gain. (a) Mode 1, (b) Mode 2, (c) Mode 3, and (d) Mode 4.

Figure 7 depicts the simulated and measured gains of the proposed antenna in all modes. Measured and simulated gain values are in better agreement. In Modes 1, 2, and 3, optimal gain values are 2.5 dBi, 1.6 dBi, 1.9 dBi, 1.8 dBi, 2.3 dBi, and in mode-4 it is 5.9 dBi.

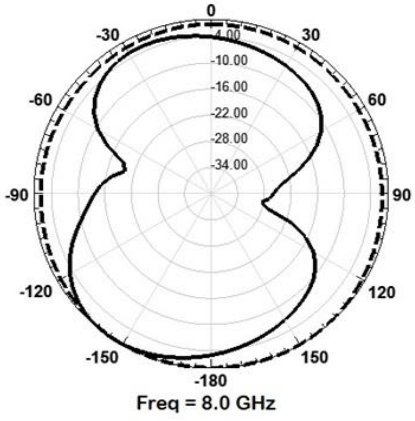

Mode-1

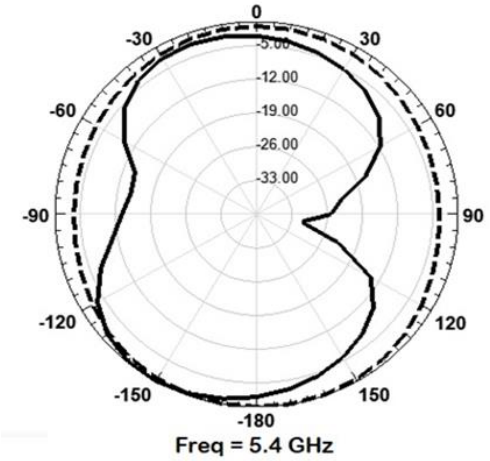

Mode-4

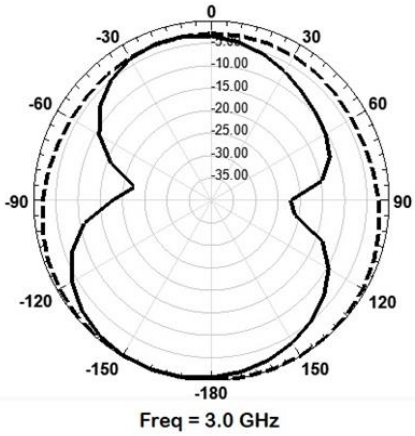

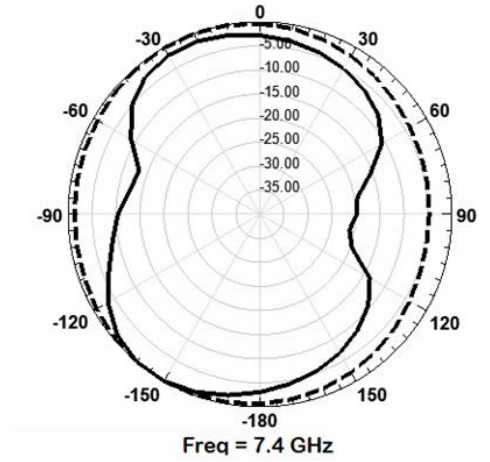

Mode-2

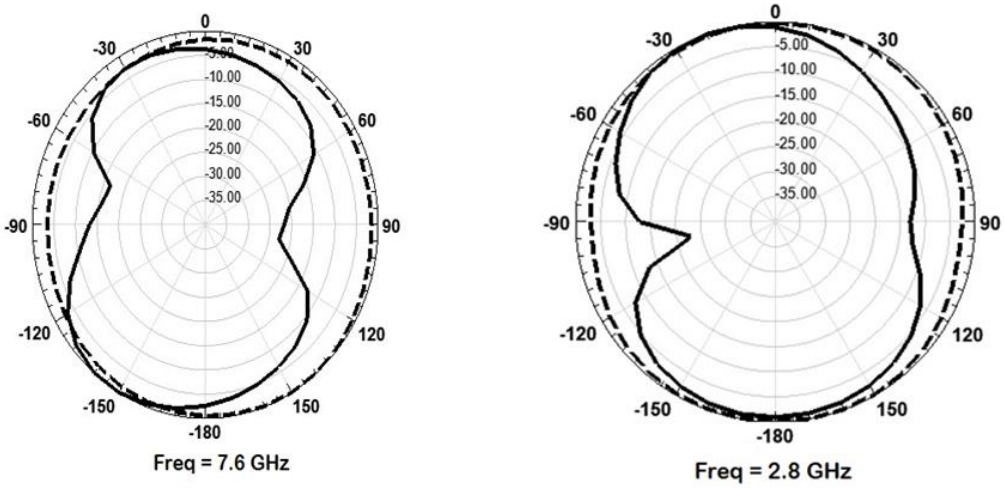

Mode-3

Figure 8. Simulated radiation pattern plots in the E-plane (X-Y) and H-plane (X-Z) of several modes.

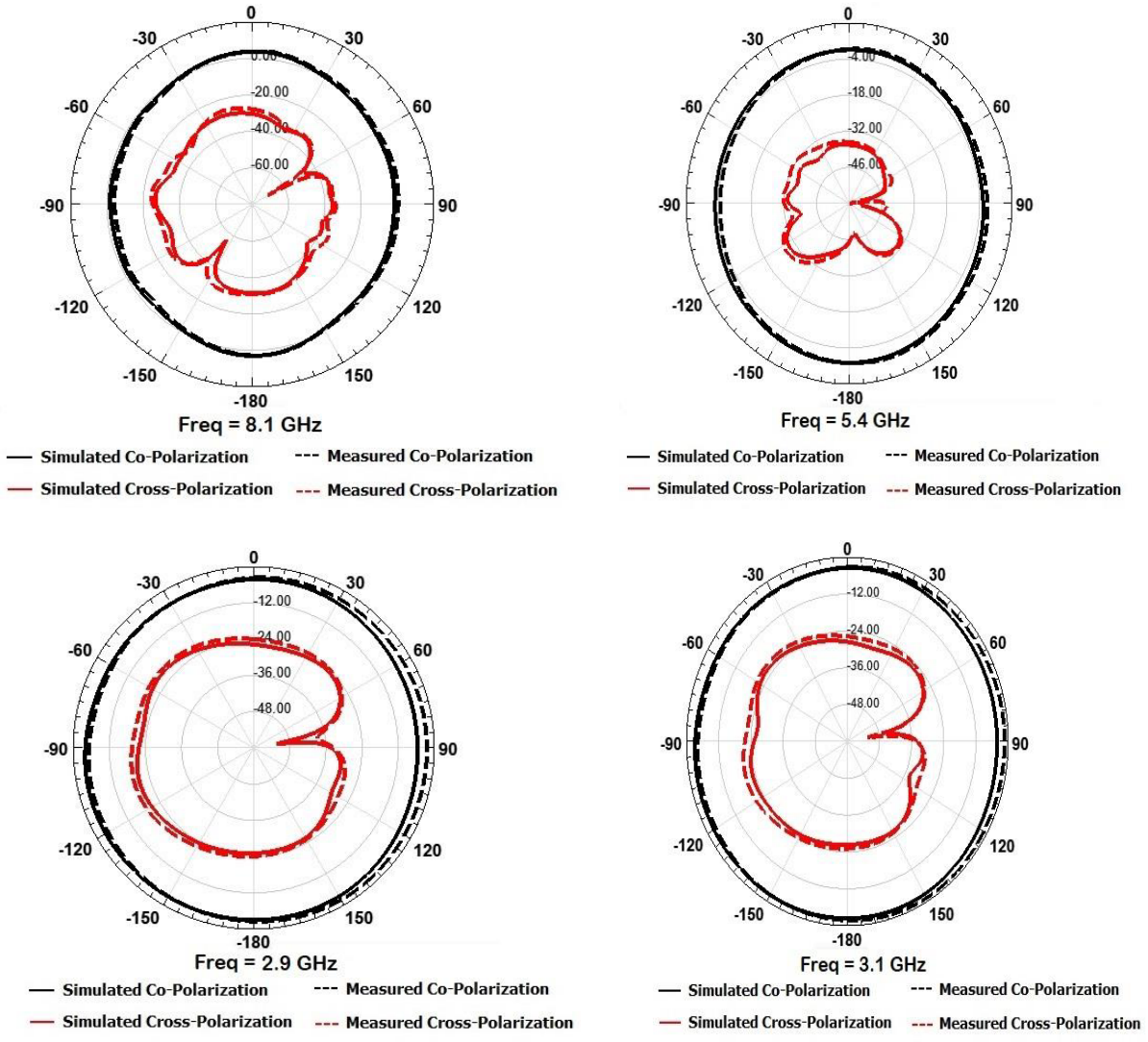

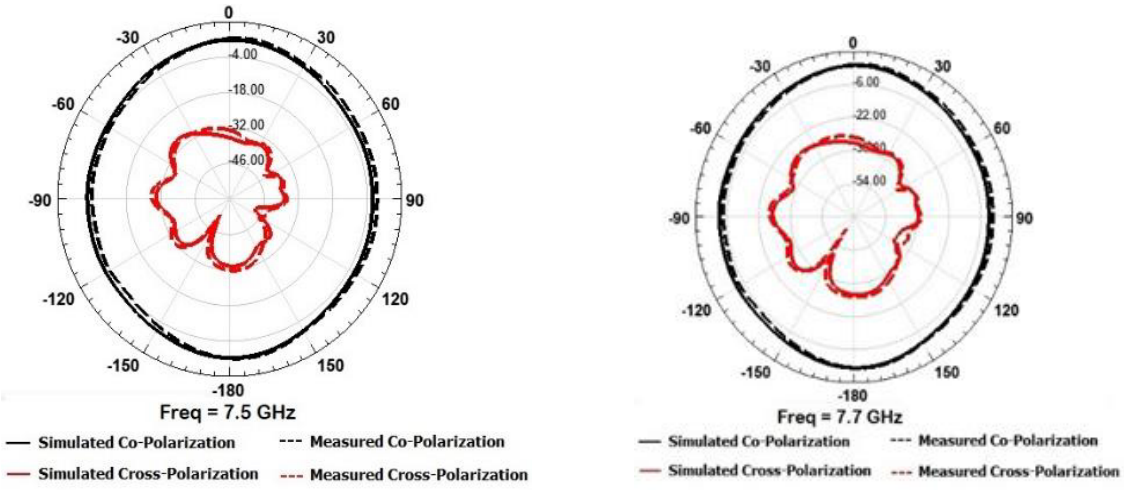

Figure 9. Co-polarization and cross-polar radiation patterns in both major planes of several modes.

The suggested Hexa-band antenna omnidirectional emission pattern is intriguing. Its prominent pattern in the H-plane results in an 8-shape and in the E-plane dominating zero lobes developing at a 90-degree angle across all frequency bands (refer to Figure 8). For all resonating modes, the radiation pattern is steady. That is one of the primary benefits of the proposed antenna.

Figure 9 shows the simulated and measured co-polarization and cross-polarization for both the E- and H-planes. In the co-polarization state, the antenna emits significantly in both planes. In contrast, antenna gain is significantly negative, resulting in extremely poor radiation in the E- and H-planes in the cross-polarization state.

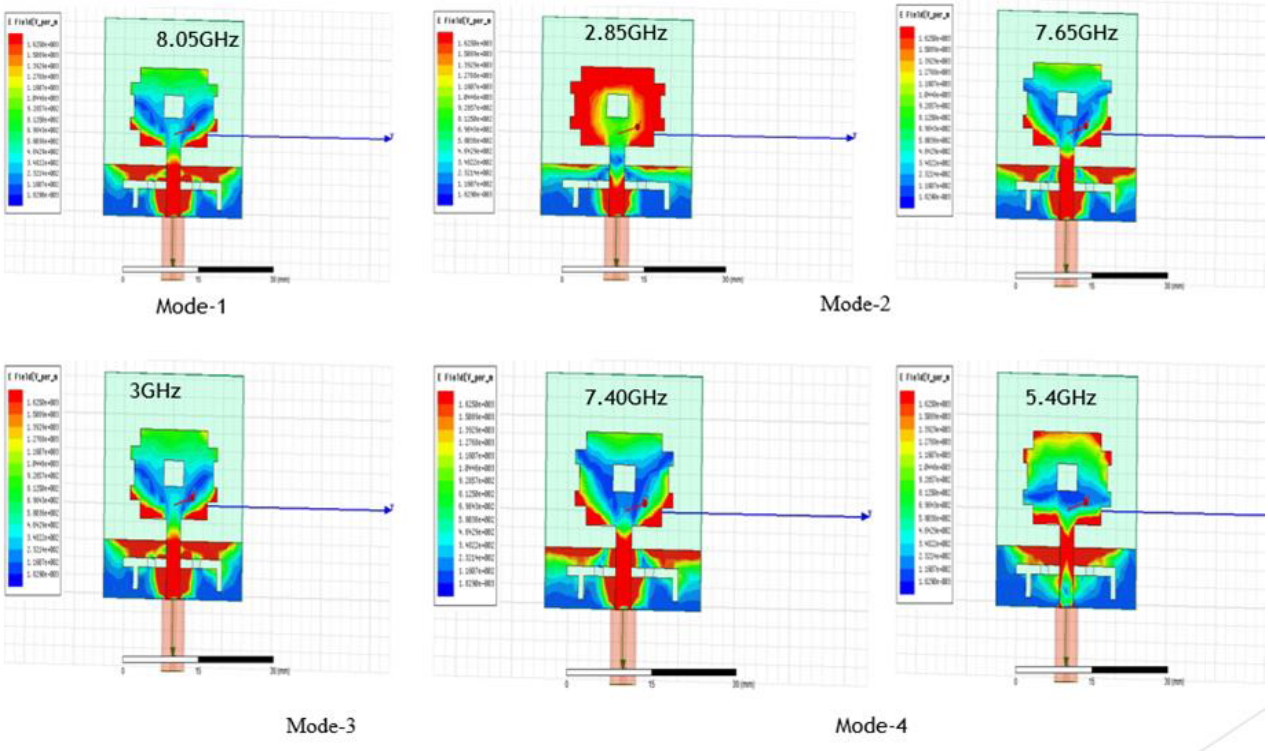

Figure 10. Distribution of surface current in different modes.

3.3. Surface Current Distribution

Reconfigurability essentially involves changing the current distribution within the radiating element, which can be realised by employing various switches, such as PIN diode. Surface current is a type of current that appears on the surface of the patch and the ground. The dispersion of surface current is the greatest in Mode-1 on the principal radiator, which donates radiation at 8 GHz. The maximum distribution of current is on the patch of Mode-2, which donates radiation at 2.85 GHz. Surface current in Mode-4 reports an increase in resonant length, causing the resonance to switch to 5.45 GHz. Figure 10 depicts the current distribution of radiating elements at various operating bands. This surface current shows that as the resonant frequency increases, the length of the donating resonant channel decreases, indicating that frequency is inversely proportional to resonant length.

Table 3 summarises the proposed antenna performance. According to simulations and experiments, the antenna works in a variety of commercial bands. Table 4 shows the frequency band and its applications, including WLAN/Bluetooth (2.4–2.5 GHz), LTE/4G (2.3–2.7 GHz), S-band (2–4 GHz), Radio Navigation (2.7–2.9 GHz), and 5G/sub-6 (3.3–4.9 GHz) applications.

The antenna under consideration is compared to recent state-of-the-art antennas to more effectively demonstrate its superiority and highlight its uniqueness. Tables 5 and 6 compare the compactness, operating passbands, frequency range, fractional bandwidth, and radiation efficiency of the structure to that of other structures. All these factors favour the examined antenna, particularly with a wide passband reconfiguration. The examined antenna is substantially denser in terms of dimensions than the antennas reported in [18, 21–34]. The impedance bandwidth obtained from the studied antenna is

Table 3. Summary of the antenna's performance.

Sr. no.	Switch Conditions	Freq. GHz	Return Loss (dB)	VSWR	BW in MHz	BW in per.	Gain [dB]	Efficiency (%)	Characteristics
1.	Both Switch OFF (D1 & D2)	8.10	−12.17	1.65	1980	28.69	2.5	89.3	Single Band
2.	Switch (D1) ON and Switch (D2) OFF	7.70	−16.41	1.35	2880	44.30	1.9	89.7	Narrowband and wideband
		2.90	−11.92	1.67	1090	16.76	1.6	91.3	
3.	Switch (D1) OFF and Switch (D2) ON	7.50	−17.84	1.29	2900	44.15	2.3	87.5	Wideband and narrowband
		3.10	−13.20	1.56	1080	16.43	1.8	93.4	
4.	Both Switch ON (D1& D2)	5.45	−36.63	1.03	5330	82.07	5.8	86.8	Wide Band

Table 4. Frequency band and its applications.

Sr. No	Freq [GHz]	Applications
1.	2.9 (2.3–3.3)	WLAN/Bluetooth (2.4–2.5 GHz) LTE/4G (2.3–2.7 GHz)
2.	3.10 (2.4–3.5)	S-band Communication (2–4 GHz) Aeronautical Radio Navigations (2.7–2.9 GHz)
3.	5.45 (2.4–7.8)	5G Mobile communication (3.3–4.9 GHz) WLAN (5.0–6.0 GHz) Wi-MAX (3.3–3.8 GHz)
4.	7.50 (5.7–8.7)	INSAT C-band Applications (6.72–7.02 GHz)
5.	7.670 (6.0–8.8)	X-band Satellite communication (7.9–8.4 GHz)
6.	8.10 (6.9–8.9)	International Telecommunication Union Fixed wireless system (ITU) (7.725–8.4 GHz)

Table 5. Dissimilarities between the proposed antenna and other published multiband antennas.

Ref.	Dimensions (mm^3)	Number of Operating Bands	Frequency Bands (GHz)	Bandwidth in MHz	Gain in dBi	Radiation Efficiency (%)
[27]	$40 \times 35 \times 1.6$ Dielectric permittivity-4.4	3	2.45, 3.5, 5.4	490–1360	1.92–3.02	76.4–86.5
[28]	$60 \times 60 \times 1.6$ Dielectric permittivity-4.4	5	2.4, 4.26, 4.32, 4.58, 5.76	60–170	1.31–2.77	—
[29]	$53 \times 35 \times 1.6$ Dielectric permittivity-4.4	3	2.45, 3.50, 5.20	147–1820	1.7–3.4	85–90
[30]	$40 \times 22 \times 1.6$ Dielectric permittivity-4.4	4	2.45, 5.13, 3.49, 5.81	750–1260	1.72–2.96	76.4–92
[31]	$39 \times 37 \times 1.6$ Dielectric permittivity-4.4	3	2.4, 5.4, 3	550–1220	1.27–3.8	> 90
[32]	$37 \times 35 \times 1.6$ Dielectric permittivity-4.4	4	2, 3.4, 2.4, 3.1	200–960	1.76–1.98	> 85
[33]	$40 \times 35 \times 1.6$ Dielectric permittivity-4.4	3	2.45, 3.5, 5.2	330–1250	1.48–3.26	84–93.5
[34]	$40 \times 35 \times 1.6$ Dielectric permittivity-4.4	6	2.10, 2.40, 3.35, 3.50, 5.28, 5.97	335–1220	1.92–3.8	92.5–97
Proposed work	**$28 \times 25 \times 1.53$ Dielectric permittivity-4.2**	**6**	**2.9, 3.10, 5.45, 7.50, 7.70, 8.10**	**1080–5300**	**1.6–5.8**	**86.8–93.4**

Table 6. The proposed antenna's performance in comparison to other published frequency reconfigurable works.

Ref/Journal	Dimension (mm^3)	Frequencies (GHz)	No. of bands	Total PIN diodes	Bandwidth in GHz	Fractional Bandwidth (%) or MHz Bandwidth	Efficiency	Characteristics
[21] Hindawi International Journal of Antennas and Propagation 2018	$40 \times 30 \times 1.6$ Dielectric permittivity-4.4	3.45 3.50 3.65 3.75 3.95 4.05	6	4	(3.27–3.80) (3.38–3.93) (3.31–3.88) (3.66–4.30) (3.70–4.21) (3.68–4.22)	14.09 15.04 15.07 15.09 12.80 13.60	69 to 80%	Narrow Band
[22] IETE Journal of Research 2018	$20 \times 24 \times 0.8$ Dielectric permittivity-2.2 (Roger)	3.6, 4.3, 5.5, 6.5, 6.9	5	2	4.19–4.48, 5.98–6.4, 3.42–4.0, 5.4–5.68, 6.8–7.0	577, 281, 285, 411 223	80 to 83%	Narrow Band
[23] AEU-International Journal of Electronics and communication engineering 2018	$33 \times 16 \times 1.6$ Dielectric permittivity-4.5	2.10 2.40 3.50 4.15 4.80 5.20	6	3	(1.98–2.20) (2.25–2.53) (3.10–2.85) (3.85–4.38) (3.90–5.82) (4.90–5.45)	9.35 13.20 21.49 11.71 41.56 9.35	80 to 96%	Narrow Band And Wideband

Ref/Journal	Dimension (mm^3)	Frequencies (GHz)	No. of bands	Total PIN diodes	Bandwidth in GHz	Fractional Bandwidth (%) or MHz Bandwidth	Efficiency	Characteristics
[18] Wireless Personal Communications Springer 2020	$37 \times 47 \times 1.6$ Dielectric permittivity-4.4	1.36, 1.80 3.00, 3.9, 5.00, 6.4, 7.4, 7.9, 8.2, 8.4, 8.6	10	3	NA	2.57 1.11 3.3 5 8 1.7 5 11 3.6 5.5 2.3	NA	Narrow Band
[24] MDPI Micro machines 2021	$40 \times 32 \times 1.6$ Dielectric permittivity-4.3	5 3.5 2.6 6.5 2.1 5.6, 1.8, 4.8, 6.4	9	4	4.21–5.61 3.05–4.42 2.40–2.90 6.27–6.94 1.95–2.25 5.41–5.86 1.71–1.90 4.55–5.13	10.5 to 28%. (190–1400 MHz)	70 to 84%	Narrow and Wideband
[25] International Journal of Electronics Letters 2020	**$40 \times 48 \times 1.6$ Dielectric permittivity-4.4**	3.1 to 8.9	5	2	3.21–3.84 4.98–5.66 5.95–6.76 32–10.14 6.17–6.78 8.06–10.17 8.06–10.17	630 to 1820 MHz	79 to 95%	Narrow and wideband
[26] MDPI Applied sciences 2021	**$30 \times 30 \times 1.9$ Dielectric permittivity-10.2 (RT6010)**	**1.8 to 4.**	**4**	**2**	**2.1 to 4.47**	–	**Less than 86%**	**Narrow band**
Proposed work	**$28 \times 25 \times 1.53$ Dielectric permittivity-4.2**	**2.90 3.10 5.45 7.50 7.70 8.10**	**6**	**2**	**(2.3–3.3)1090 (2.3–3.6)1080 (2.4–7.8)5300 (5.7–8.9)2900 (6.0–8.8)2880 (6.8–8.9)1980**	**16.76 16.43 82.07 44.15 44.30 28.69**	**86 to 94 %**	**Narrow Band Wideband And UWB**

as per the requirements given by the FCC for 5G applications, which is 25% of the central frequency. The most noticeable difference between this antenna and other candidate antennas is its narrowband and wideband properties, which make it suitable for 5G/sub-6 GHz (3.3–4.9 GHz) and many wideband applications.

4. CONCLUSION

In this study, a compact six-band DGS-based frequency reconfigurable antenna and its experimental validation are provided. At the ground plane, the design incorporates an F-shape DGS. To gain reconfigurable properties, two RMP1320 PIN diodes are inserted into the F-shaped DGS. Depending on the ON and OFF states of the switches, the antenna operates over a wide frequency range, ranging from 2.3 to 8.9 GHz. This antenna supports narrowband, wideband, and UWB properties. Under

different working conditions, the antenna provided satisfactory return loss, VSWR, radiation patterns, and gain values. The impedance bandwidths obtained for various bands vary from 16.43 to 82.07%, and the radiation efficiency is 86.8% to 93.4%. The benefits of this antenna are its compactness, low cost, consistent omnidirectional radiation pattern, and ease of construction. Because of these benefits, the proposed antenna is an excellent candidate for WLAN/Bluetooth (2.4–2.5 GHz), LTE/4G (2.3–2.7 GHz), S-band Communication (2–4 GHz), Radio Navigation (2.7–2.9 GHz), 5G sub-6 GHz mobile communication (3.3–4.9 GHz), Wi-MAX (3.3–3.8 GHz), WLAN (5.0–6.0 GHz), and INSAT Applications (6.72–7.02 GHz).

5. FUTURE PROSPECTS

The use of MIMO antennas in wireless communication systems is becoming more common due to their increased reliability and efficiency. Because of low cross-polarization, steady radiation pattern, wide bandwidth, and high efficiency, the suggested design can be used to build frequency-reconfigurable MIMO antenna systems for 5G applications.

ACKNOWLEDGMENT

The authors would like to thank the Department of Electronics and Communication Engineering, Dayananda Sagar University, Bangalore, Karnataka, India for the timely help and support for carrying out this work.

Conflict of Interest

The authors declare that they have no known competing financial interests or personal relationships that could have appeared to influence the work reported in this paper.

Data Availability Statement

The datasets generated or analysed during the current study are available from the corresponding author on reasonable request.

REFERENCES

1. Li, T., Y. Dong, P. Fan, and K. B. Letaief, "Wireless communications with RF-based energy harvesting: From information theory to green systems," *IEEE Access*, Vol. 5, 27538–27550, 2017.
2. Guo, Y. J., P.-Y. Qin, S. L. Chen, W. Lin, and R. W. Ziolkowski, "Advances in reconfigurable antenna systems facilitated by innovative technologies," *IEEE Access*, Vol. 6, 5780–5794, 2018.
3. Khaleel, H., *Innovation in Wearable and Flexible Antennas*, Wit Press, Boston, MA, USA, 2014.
4. Awan, W. A., N. Hussain, and T. T. Le, "Ultra-thin flexible fractal antenna for 2.45 GHz application with wideband harmonic rejection," *AEU-Int. J. Electron Commun.*, Vol. 110, Oct. 2019, Art. no. 152851.
5. Global update on 5G spectrum (2019). https://www.qualcomm.com/media/documents/files/spectrum-for-4g-and-5g.pdf.
6. Mudda, S. and K. M. Gayathri, "Frequency reconfigurable ultra-wide band MIMO antenna for 4G/5G portable devices applications: Review," *International Journal on Emerging Technologies*, Vol. 11, No. 3, 486–490, 2020.
7. Li, Y., W. Li, and Q. Ye, "A reconfigurable triple-notch-band antenna integrated with defected microstrip structure band-stop filter for ultra-wideband cognitive radio applications," *International Journal of Antennas and Propagation*, 2013.
8. Gheethan, A. E. and D. E. Anagnostou, "Broadband and dual-band coplanar folded-slot antennas (CFSAs) [Antenna designer's notebook]," *IEEE Antennas Propag. Mag.*, Vol. 53, No. 1, 80–89, 2011.
9. Balanis, C. A., *Antenna Theory: Analysis and Design*, 3rd Edition, Wiley, Hoboken, 2005.

10. Mudda, S., K. M. Gayathri, and M. Mudda, "Compact high gain microstrip patch multi-band antenna for future generation portable devices communication," *2021 International Conference on Emerging Smart Computing and Informatics (ESCI)*, 471–476, 2021, doi: 10.1109/ESCI50559.2021.9396776.
11. Shynu, S. V., G. Augustin, C. K. Aanandan, P. Mohanan, and K. Vasudevan, "A reconfigurable dual frequency slot-loaded microstrip antenna controlled by PIN diodes," *Microwave Optical Technology Letters*, Vol. 44, 374–376, 2005.
12. Jin, G., C. Deng, J. Yang, Y. Xu, and S. Liao, "A new differentially-fed frequency reconfigurable antenna for WLAN and sub-6 GHz 5G applications," *IEEE Access*, Vol. 7, 56539–56546, 2019.
13. Khan, M. F., S. A. Shah, and S. Ullah, "Dual-band frequency reconfigurable microstrip patch antenna on the wearable substrate for Wi-Fi and Wi-MAX applications," *Technical Journal*, Vol. 22, 35–40, University of Engineering and Technology, Taxila, Pakistan, 2017.
14. Xin, G. L. and J. P. Xu, "Wideband miniature G-shaped antenna for dual-band WLAN applications," *Electronics Letters*, Vol. 43, No. 24, 1330–1332, Nov. 22, 2007.
15. Jin, G. P., D. L. Zhang, and R. L. Li, "Optically controlled reconfigurable antenna for cognitive radio applications," *Electronics Letters*, Vol. 47, No. 17, 948–950, Aug. 18, 2011.
16. Rajagopalan, H., J. M. Kovitz, and Y. Rahmat Samii, "MEMS reconfigurable optimized E-shaped patch antenna design for cognitive radio," *IEEE Transactions on Antennas and Propagation*, Vol. 62, No. 3, 1056–1064, 2014.
17. Chaouche, Y. B., I. Messaoudene, I. Benmabrouk, M. Nedil, and F. Bouttout, "Compact coplanar waveguide-fed reconfigurable fractal antenna for switchable multiband systems," *IET Microw. Antennas Propag.*, Vol. 13, 1–8, 2018.
18. Sathikbasha, M. J. and V. Nagarajan, "DGS based multiband frequency reconfigurable antenna for wireless applications," *International Conference on Commun. and Signal Processing (ICCSP)*, 0908–0912, 2019, doi: 10.1109/ICCSP.2019.8698093.
19. Abdulraheem, Y. I., G. A. Oguntala, A. S. Abdullah, H. J. Mohammed, R. A. Ali, R. A. Abd-Alhameed, and J. M. Noras, "Design offrequency reconfigurable multiband compact antenna using two PIN diodes for WLAN/WiMAX applications," *IET Microw. Antennas Propag.*, Vol. 11, 1098–1105, 2017.
20. Ali, T., M. M. Khaleeq, and R. C. Biradar, "A multiband reconfigurable slot antenna for wireless applications," *AEU Int. J. Electron. Commun.*, Vol. 84, 273–280, 2018.
21. Han, L., C. Wang, W. Zhang, R. Ma, and Q. Zeng, "Design of frequency- and pattern-reconfigurable wideband slot antenna," *International Journal of Antennas and Propagation*, Vol. 2018, Article ID 3678018, 7 pages, 2018, https://doi.org/10.1155/2018/3678018.
22. Ahmad, A., F. Arshad, S. I. Naqvi, Y. Amin, H. Tenhunen, and J. Loo, "Flexible and compact spiral-shaped frequency reconfigurable antenna for wireless applications," *IETE Journal of Research*, 2018, doi: 10.1080/03772063.2018.1477629.
23. Shah, I. A., S. Hayat, A. Basir, M. Zada, S. A. A. Shah, and S. Ullah, "Design and analysis of a hexa-band frequency reconfigurable antenna for wireless communication," *International Journal of Electronics and Communications*, 2018, doi: https://doi.org/10.1016/j.aeue.2018.10.012.
24. Dildar, H., F. Althobiani, I. Ahmad, W. U. R. Khan, S. Ullah, N. Mufti, S. Ullah, F. Muhammad, M. Irfan, and A. Glowacz, "A design and experimental analysis of multiband frequency reconfigurable antenna for 5G and sub-6 GHz wireless communication," *Micromachines*, Vol. 12, 32, 2021, https://doi.org/10.3390/mi12010032.
25. Khan, T. and M. U. Rahman, "Design of low-profile frequency reconfigurable antenna for multiband applications," *International Journal of Electronics Letters*, 2021, doi: 10.1080/21681724.2020.1818836.
26. Ghaffar, A., X. J. Li, W. A. Awan, S. Iffat Naqvi, N. Hussain, B.-C. Seet, M. Alibakhshikenari, F. Falcone, and E. Limiti, "Design and realization of a frequency reconfigurable multimode antenna for ISM, 5G-sub-6-GHz, and S-band applications," *Appl. Sci.*, Vol. 11, 1635, 2021, https://doi.org/10.3390/app11041635.

27. Saikia, B., P. Dutta, and K. Borah, "Design of a frequency reconfigurable microstrip patch antenna for multiband applications," *Proceedings of the 5th International Conference on Computers & Management Skills (ICCM 2019)*, Arunachal Pradesh, India, Dec. 15–16, 2019.
28. Ulla, S., S. Hayat, A. Umar, A. Ali, and J. A. Flint, "Design, fabrication, and measurement of triple-band frequency reconfigurable antennas for portable wireless communications," *AEU-Int. J. Electron. Commun.*, Vol. 81, 236–242, 2017.
29. Iqbal, A., S. Ullah, U. Naeem, A. Basir, and U. Ali, "Design, fabrication, and measurement of a compact frequency reconfigurable modified T-shape planar antenna for portable applications," *J. Electr. Eng. Technol.*, Vol. 12, 1611–1618, 2017.
30. Ullah, S., I. Ahmad, Y. Raheem, S. Ullah, T. Ahmad, and U. Habib, "Hexagonal shaped CPW feed based frequency reconfigurable antenna for WLAN and sub-6 GHz 5G applications," *Proceedings of the International Conference on Emerging Trends in Smart Technologies (ICETST)*, Karachi, Pakistan, Mar. 26–27, 2020; IEEE, Piscataway, NJ, USA, 2020.
31. Shah, I. A., S. Hayat, I. Khan, I. Alam, S. Ullah, and A. Afridi, "A compact tri-band and 9-shape reconfigurable antenna for WiFi WiMAX and WLAN applications," *Int. J. Wirel. Microw. Technol. (IJWMT)*, Vol. 6, 45–53, 2016.
32. Ullah, S., A. Shaheen, B. A. Khan, and J. A. Flint, "A multi-band switchable antenna for Wi-Fi, 3G advanced, WiMAX, and WLAN wireless applications," *Int. J. Microw. Wirel. Technol.*, Vol. 10, 991–997, 2018.
33. Shah, S. A., M. F. Khan, S. Ullah, A. Basir, U. Ali, and U. Naeem, "Design and measurement of planar monopole antennas for multiband wireless applications," *IETE J. Res.*, Vol. 63, 194–204, 2017.
34. Dildar, H., F. Althobiani, W. U. R. Ahmad Khan, S. Ullah, N. Mufti, S. Ullah, F. Muhammad, M. Irfan, and A. Glowacz, "Design and experimental analysis of multiband frequency reconfigurable antenna for 5G and sub-6 GHz wireless communication," *Micromachines*, Vol. 12, 32, 2021, https://doi.org/10.3390/mi12010032.